Provided for non-commercial research and education use.
Not for reproduction, distribution or commercial use.

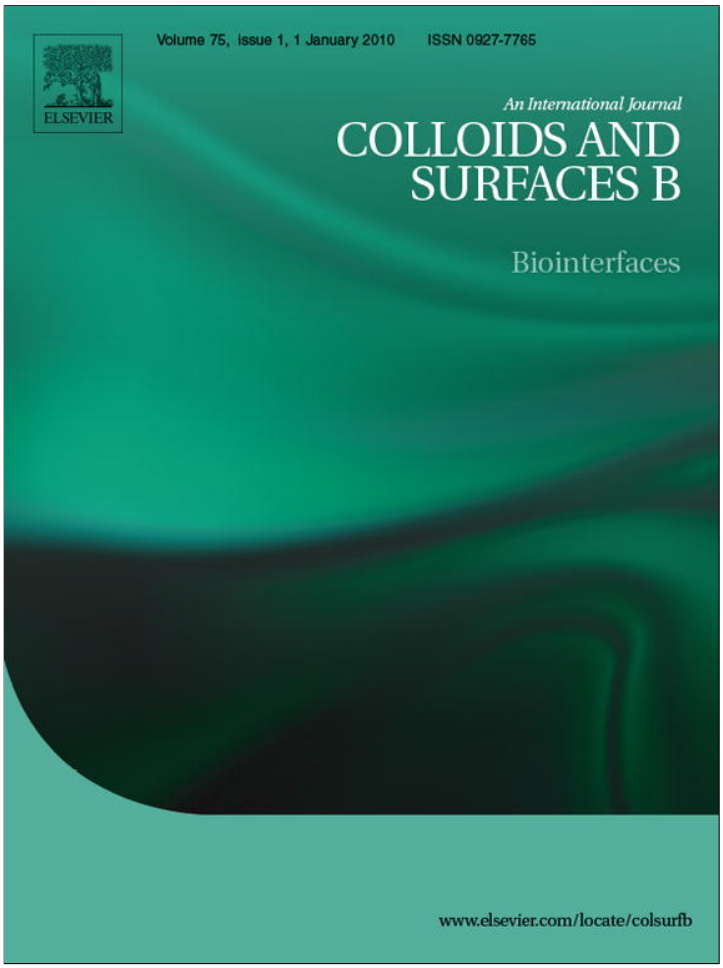

This article appeared in a journal published by Elsevier. The attached copy is furnished to the author for internal non-commercial research and education use, including for instruction at the authors institution and sharing with colleagues.

Other uses, including reproduction and distribution, or selling or licensing copies, or posting to personal, institutional or third party websites are prohibited.

In most cases authors are permitted to post their version of the article (e.g. in Word or Tex form) to their personal website or institutional repository. Authors requiring further information regarding Elsevier's archiving and manuscript policies are encouraged to visit:

http://www.elsevier.com/copyright

Author's personal copy

Colloids and Surfaces B: Biointerfaces 75 (2010) 57–66

Contents lists available at ScienceDirect

Colloids and Surfaces B: Biointerfaces

journal homepage: www.elsevier.com/locate/colsurfb

Phosphatidylcholine/vegetable oil pseudo-binary mixtures at the air–water interface: Predictive formulation of oil blends with selected surface behavior

Benjamín Caruso[a,c], Damián M. Maestri[b,c], María A. Perillo[a,c,*]

[a] Biofísica-Química, Cátedra de Química Biológica, Universidad Nacional de Córdoba, Av. Vélez Sarsfield 1611, X5016GCA Córdoba, Argentina
[b] IMBIV-CONICET-Cátedra de Química Orgánica, Depto. de Química, Universidad Nacional de Córdoba, Av. Vélez Sarsfield 1611, X5016GCA Córdoba, Argentina
[c] ICTA, Facultad de Ciencias Exactas, Físicas y Naturales, Universidad Nacional de Córdoba, Av. Vélez Sarsfield 1611, X5016GCA Córdoba, Argentina

ARTICLE INFO

Article history:
Received 5 June 2009
Received in revised form 4 August 2009
Accepted 6 August 2009
Available online 14 August 2009

Keywords:
Phosphatidylcholine
Vegetable oils
Monolayers
Surface parameters
Chemical composition

ABSTRACT

The present work is an attempt to define how to formulate oil blends with an expected surface behavior using easily accessible data such as chemical compositions. Hence, we determined average surface properties of triglycerides (TG) from olive (O), soybean (S), and walnut (W) oils self-organized in Langmuir films alone or in pseudo-binary mixtures with phosphatidylcholines (PC).

Collapse pressure (π_c), compressibility modulus (K) and molecular area at the closest packing (A_{min}) were determined from π-mean molecular area (Mma) isotherms. The π_c-composition phase diagrams of TG–PC mixtures provided information about oils solubility limit with PCs in the monolayer phase. A thermodynamic equilibrium model was fitted to the line joining points of monolayer–$TG_{liquid\ phase}$ coexistence and allowed to obtain interaction parameters, ω, which consistently with those of excess surface energy (ΔG_{ex}) and Mma deviations from ideality, contributed to describe interfacial intermolecular interactions. Oil molar fractions (x_{TG}) for TGs–PCs self-assembling into vesicles were estimated from x_{TG} values at $\pi_c \cong 30$ mN/m (equilibrium π of bilayers), which resulted higher in egg PC (0.15, 0.2, 0.15 for O, S and W, respectively) than in dipalmitoyl-PC (0.125, 0.075, 0.1).

Principal component analysis performed on surface parameters, grouped S and W separated from O. This result was mainly influenced by variables estimating the effect of unsaturation degrees of fatty acids sterified at TGs, A_{min} and π_c.

Peanut oils surface data interpolated in π_c-C16/C18 and A_{min}–DBI correlation lines obtained with O–S mixtures (TG_{mix}) and with TG_{mix}–PC supported C16/C18 ratio and DBI as predictors to formulate oil blends with selected surface behavior.

© 2009 Elsevier B.V. All rights reserved.

1. Introduction

Triacylglycerols, also named triglycerides (TGs), are amphiphiles widely distributed in nature, which can be found either in animals or plants. Many TGs are in the form of edible animal fat and vegetable oils and can be used in food preparations. Moreover, these molecules have important technical applications in medicine, cosmetic, pharmaceutical and food industries [1].

Food formulations containing lipids and oils are in increasing demand for the preparation of low-fat products such as cream sauces, salad dressings and liqueurs. Furthermore, flavors, essential oils and a number of nutraceuticals such as carotenes, lutein, fatty acids, flavonoids, plant stanols and phytoestrogens are water-insoluble materials that display some affinity for oil what make them feasible to be formulated in an oil–water dispersion such as an emulsion or a microemulsion [2].

The chemical composition of TGs plays an important role in determining the technological and physiological behavior of oils. Sensorial food properties such as the palatability, transparency or homogeneous aspect of an emulsion will be highly dependent on the solubility of their component fats. Although a few microemulsion systems based on TGs have been reported in the literature, vegetable oils containing long-chain fatty acids, mainly C16 and C18, result in large TGs structures that are difficult to solubilize into microemulsions systems and often form liquid crystalline

Abbreviations: A_{min}, minimal molecular area; DBI, Double Bond Index; DI, deviation from ideality; ΔG_{ex}, excess Gibbs free energy; HOP, high-oleic peanut oil; K, compressional modulus, at transition (K_T) or collapse (K_C) points; Mma, mean molecular area; MMM, mean molecular mass; NP, normal peanut oil; O, olive oil; PC, phosphatidylcholine; EPC, egg-yolk phosphatidylcholine; dpPC, dipalmitoylphosphatidylcholine; PCA, principal component analysis; π, lateral surface pressure, at collapse (π_c) or transition (π_T) points; SO, S_S and S_N, oils' solubilities in PC; S, soybean oil; TGs, triacylglycerols; TG_{mix}, oils' mixtures; W, walnut oil; ω, lateral interaction value.

* Corresponding author at: ICTA, Facultad de Ciencias Exactas, Físicas y Naturales, Universidad Nacional de Córdoba, Av. Vélez Sarsfield 1611, X5016GCA Córdoba, Argentina. Fax: +54 351 4344983.
E-mail address: mperillo@efn.uncor.edu (M.A. Perillo).

0927-7765/$ – see front matter © 2009 Elsevier B.V. All rights reserved.
doi:10.1016/j.colsurfb.2009.08.014

Author's personal copy

mesophases [3]. Differences in the acyl chains of the constituent TGs have also been shown to affect the clearance from plasma of chylomicron-like emulsions injected intravenously [4], to modulate lipase activity [5,6] and consequently to affect the digestibility of TGs based foods. This is related with the fact that knowledge of the concentration and state of apolar lipids in surface phases is important because lipolytic enzymes, such as lipases, act at the surface of the substrate particle, not its core [7].

Physical and functional properties of emulsions, liposomes and membrane systems containing TGs are closely related with the molecular packing and structure. The aliphatic chain–chain interactions are critical factors for the determination of physical properties such as softness and flexibility of the fats and lipids. In turn, their packing conditions depend on the chemical nature of their fatty acid moieties: chain length, parity (odd or even), unsaturation (*cis* or *trans)*, etc. [8]. Reducing the acyl chain length of the *sn*-2 chain and increasing the unsaturation of sterified fatty acids will effectively reduce the total van der Waals surface contacts among adjacent hydrocarbon chains [9].

Surface organization is defined by several factors in a combined manner, mainly topology and the packing and mobility of molecular components. In tridimensional systems like liposomes or emulsion particles, these properties are mutually affected. Conversely, in monomolecular layers at the air–water interface (monolayers) it is possible to maintain a constant planar topology and to control the molecular packing simultaneously. Studies on monolayers revealed that even in simple samples the bi-dimensional phase behavior may be complex. TGs with long fatty acids exhibit a rich polymorphism that has been thoroughly studied in Langmuir monolayers [10]. Furthermore, monolayer studies with simple mixtures of pure TGs and phosphatidylcholines (PC) revealed that the proportion of TG remaining in the monolayer phase at lateral surface pressures (π) above the collapse pressure (π_c) depended on the fatty acid composition of the TG (e.g. more OOO than OOS or SOO was retained where O and S here represent oleic and stearic acids, respectively) [4]. If the chain length of one or more acyl chains of the TG is decreased substantially, the maximum solubility of the TG in egg PC may differ significantly from that of the long-chain TG. As measured by NMR methods, the medium-chain TG trioctanoin was soluble to the extent of approximately 14 mol.%, more than 3 times that of triolein (OOO) or tripalmitin (PPP). The solubility of TG with two long-chains and a short chain was intermediate between those of long-chain TG (PPP or OOO) and trioctanoin ([11] and references therein). These differences could underlie the effects on metabolism of saturated chains in triacylglycerols emulsions [4] and preclude a strong influence of fatty acid composition on the surface stability and drug vehiculization ability of the nanoparticles (either liposomes or emulsions) formulated with TGs.

It is important to note that studies on monolayers with complex mixtures such as natural oils lead to define average values for the surface parameters which in turn may not be straightforwardly predicted from the behavior of individual molecular components. This is due to the fact that surface parameters of molecular mixtures are the resultant of properties emerging at the supramolecular organizational level.

In the present work we describe the behavior at the air–water interface of TGs from olive (O), soybean (S) and walnut (W) oils alone or in pseudo-binary mixtures with phosphtidylcholines (PCs). This allowed studying the properties and dynamics of the intermolecular interactions in TG–PC complex mixtures in well defined conditions of composition and lateral packing and helped us to predict the mutual solubility between oils and PCs. This analysis was extended to blends prepared with convenient proportions of O and S to obtain TG mixtures (TG_{mix}) covering a wide range of double bond index (DBI) values. This allowed predicting the behavior of other natural oils such as Normal Peanut (NP) and High Oleic Peanut (HOP) oils from weighted average values of variables easily derived from their TG composition. Hence, the C16/C18 molar ratio and DBI are proposed as convenient predictors to formulate oil blends with selected surface behavior.

2. Materials and methods

2.1. Materials

Refined, bleached and deodorized soybean (S) oil was provided by Aceitera General Deheza (Córdoba, Argentina), and it was stored under N_2 at −10 °C until used. Olive (O), Walnut (W) and two varieties of peanut oils (High Oleic (HOP) and Normal (NP) Peanut oils) were extracted using manually operated pilot-plant hydraulic presses as described previously [12,13]. Crude oils thus obtained (10 g in 100 ml n-hexane) were passed through a 2 cm i.d. column filled with 70 g alumina (Al_2O_3, neutral, activity stage II, Fluka, Buchs, Switzerland) activated at 180 °C for 4 h. The TG fraction obtained from each oil was further purified using 3% of an acid activated bleaching clay as indicated elsewhere [12]. These TGs were stored at −20 °C. 1,2-Dipalmitoyl-sn-glycero-3-phosphocholine (dpPC) and L-a-phosphatidylcholine from egg (EPC) were purchased from Avanti Polar Lipids (Alabaster, Alabama). Solvents used were of analytical grade.

2.2. Oil analyses

Fatty acid compositions from O, S, W, HOP and NP oils were analyzed by gas chromatography (GC). Briefly, oils were subjected to alkaline saponification (1 M potassium hydroxide in methanol). The fatty acid methyl esters were obtained using 0.5 M sulphuric acid in methanol and analyzed by GC according to Torres and Maestri [13]. The identification of fatty acids was carried out by GC–mass spectrometry and by comparison of the retention times with those of reference compounds. This information was used to calculate the weighted mean molecular masses (MMM) required for determining solutions concentrations and mean molecular areas (Mma). MMM values were calculated as follows: $MMM = [\Sigma(\%{\cdot}MW)]/100$, where % is the percent composition of each fatty acid (Table 1) and MW is its respective molecular weight. Hence, MMM used for O, S, W, HOP, NP and EPC samples are shown in Table 1.

The Double Bond Index (DBI) was used to describe oils unsaturation level and was calculated according to Eq. (1):

$$\mathrm{DBI} = \sum \frac{(\mathrm{UF} \cdot \mathrm{DB})}{100} \quad (1)$$

where UF is the mole percent composition of each unsaturated fatty acid and DB is its respective number of double bonds.

2.3. Monomolecular layers at the air–water interface

Monomolecular layers were prepared and monitored essentially as described previously [14]. The equipment used was a Minitrough II (KSV Instruments Ltd., Finland). Between 20 and 60 μl of a $CHCl_3$:MeOH (2:1) solution of lipids was spread on an unbuffered aqueous surface at 24 ± 0.5 °C room temperature. About 5 min were allowed for the evaporation of the solvent. Lateral surface pressure (π) was measured by the Wilhelmy plate method. Reproducibility was within ±0.01 nm^2 and ±1 mN/m for molecular area and surface pressure, respectively.

2.4. Surface pressure (π) vs. area (A) isotherms

The surface behavior of dpPC, EPC, O, S and W TG fraction obtained as above mentioned were studied alone or in pseudo-binary TG–PC mixtures, at TG molar fraction (x) between 0 and 1.

Author's personal copy

Table 1
Physico-chemical properties of the triglycerides oils and phospholipids studied.

Chemical properties	Triglyceride oil					Phospholipid	
	Olive (O)	Soybean (S)	Walnut (W)	HOP	NP	dpPC	EPC
[a]Mean molecular mass	870.92	866.71	874.86	896.73	892.9	734.04	760.8
Fatty acid composition (%)							
Hexadecanoic (16:0)	16.47	10.97	6.79	4.88	9.43	100	33.95
9-Cis-hexadecenoic (16:1)	1.26	0	0	0	0	0	1
Octadecanoic (18:0)	2.12	4.1	1.8	1.69	1.69	0	10.52
9-Cis-octadecenoic (18:1)	71.77	20.45	20.3	78.62	43.53	0	31.06
9-Cis,12-cis-octadecadienoic (18:2)	7.67	54.91	55.79	5.79	36.51	0	17.72
9-Cis,12-cis,15-cis-octadecatrienoic (18:3)	0.69	7.85	15.5	0	0	0	0
Eicosanoic (20:0)	<0.1	0.35	<0.1	0.96	0.86	0	0
11-Cis-eicosenoic (20:1)	<0.1	0.27	0.24	2.82	1.94	0	0
20:2	0	0	0	0	0	0	0.22
20:3	0	0	0	0	0	0	.025
20:4	0	0	0	0	0	0	3.1
Docosanoic (22:0)	0	0.3	0	2.69	2.96	0	0
22:6	0	0	0	0	0	0	0.44
22:1	0	0	0	0.38	0.38	0	0
24:0	0	0	0	1.92	2.7	0	0
24:1	0	0	0	0.3	0.1	0	0
Number of carbon atoms in the sterified fatty acids							
[a]Average number ($C_{average}$)	17.68	17.66	17.96	18.243	18.18	16	17.08
[a]C16/C18	0.22	0.13	0.07	0.057	0.115	–	0.59
[a]C20/$C_{average}$	0.002	0.007	0.0038	0.041	0.031	–	0.039
Unsaturation level							
[a]Double Bound Index (DBI)	0.9054	1.5409	1.7862	0.944	1.19	0	0.837
[a]Saturated/unsaturated	0.229	0.188	0.095	0.138	0.213	–	0.82
[a]Iode Index	81.61	139.7	160.87	83.84	107.3	–	64.32
Surface properties							
[a]Collapse pressure (π_c) (mN/m)	13.1 ± 0.1	12.4 ± 0.2	12± 0.1	12.1 ± 0	12.6 ± 0.6	58	45.3
[a]Minimal molecular area (A_{min}) (Å^2)	84± 2	96± 3	102± 13	76.8 ± 2.5	89.1 ± 3.2	40	67
[a]$K_{\pi c}$ (mN/m)	58.3 ± 1.6	54 ±-1.47	53± 2.5	46.8 ± 3.7	48 ± 5.6	234	103
TG solubility in dpPC	0.125	0.075	0.1	nd	nd	–	–
TG solubility in EPC	0.15	0.20	0.15	nd	nd	–	–
ω in dpPC	−1.48 ± 0.56	−2.52 ± 0.7	−3.39 ± 0.78	nd	nd	–	–
ω in EPC	−0.22 ± 0.31	−1.86 ± 0.33	−1.91 ± 0.39	nd	nd	–	–

$K_{\pi c}$, compressional modulus at π_c; nd, not determined. Compositional data from EPC was taken from Avanti Polar Lipids (Alabaster, Alabama).
[a] Data used in PCA.

For these experiments we used a rectangular trough fitted with two barriers that were moved synchronously by electronic switching. The signal corresponding to the surface area (automatically determined by the Minitrough according to the relative position of the two compression barriers) and the output from the surface pressure transducer (measured automatically by the Minitrough with a Wilhelmy plate, platinized Pt foil 5 mm wide × 20 mm long × 0.025 mm thick) were fed into a personal computer through a serial interface using a specific software. Before each experiment the trough was rinsed and wiped with 70% ethanol and several times with bidistilled water. The absence of surface-active compounds in the pure solvents and in the subphase solution (bidistilled water) was checked before each run by reducing the available surface area to less than 10% of its original value after enough time was allowed for the adsorption of possible impurities that might have been present in trace amounts. The monolayer was compressed at a constant low rate of 5 mN m^{-1} min^{-1}. A lower compression rate (1 mN m^{-1} min^{-1}) was tested, and identical results were obtained.

Mean molecular area (Mma) at varying pressures was calculated dividing surface area by the number of molecules spread on the interface.

2.5. Thermodynamic calculations

The excess mean area of mixture, A_{ex}, at constant film pressure (π) can be expressed as:

$$A_{ex} = A_{12} - A_{id} = A_{12} - (X_1A_1 + X_2A_2) \quad (2)$$

where A_1, A_2, X_1 and X_2 are the mean molecular areas and mole fractions of single components 1 and 2, respectively, and A_{id} and A_{12} are mean molecular areas of the ideal and real mixtures of compounds 1 and 2, respectively. An $A_{ex} = 0$ means either immiscibility or ideal mixture of the components and $A_{ex} \neq 0$ represent a non-ideal mixture involving either attractive ($A_{ex} < 0$) or repulsive ($A_{ex} > 0$) interactions. The free energy involved in this interaction is the ΔG_{ex}, which can be calculated from the area under the curve of A_{ex} within a meaningful π interval (see Eq. (3), where N_0 is the Avogadro's number).

$$\Delta G_{ex} = N_0 \int_0^{\pi} [A_{12} - (X_1A_1 + X_2A_2)]d\pi \quad (3)$$

Even in ideal conditions, due to entropic contributions, any mixture of substances will involve a change in free energy identified as the ΔG_{id}:

$$\Delta G_{id} = RT(X_1 \ln X_1 + X_2 \ln X_2) \quad (4)$$

Hence, the total free energy change will be the sum of ideal and non-ideal contributions:

$$\Delta G_{mix} = \Delta G_{ex} + \Delta G_{id} \quad (5)$$

2.6. Principal component analysis

Principal component analysis (PCA) was done according to Rohlf [15]. A multidimentional, and hence unvisualizable swarm of points can be visualized when it is projected onto a space of fewer dimen-

Author's personal copy

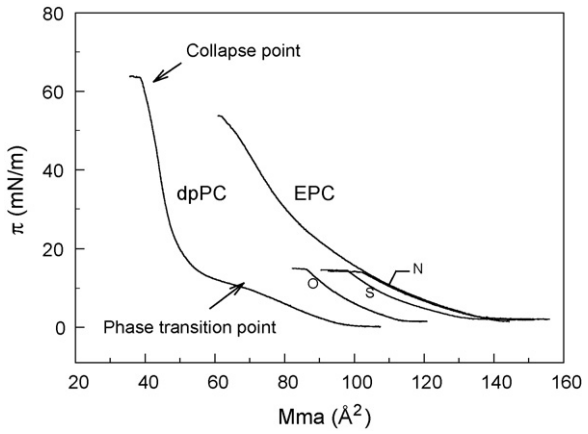

Fig. 1. Surface pressure–mean molecular area isotherms. π–Mma isotherms of the phospholipids dpPC and EPC and the TGs O, S and W oils are shown. Collapse and transition points determination are exemplified over a dpPC π–*A* compression isotherm.

sions. This can be achieved by a rigid rotation of the original axes around the origin. The new coordinates are calculated from the equation: $Y = U{\cdot}X$ where X is the original data matrix that have been previously centred and/or standardized, U is an orthogonal matrix whose rows are the eigenvectors of $R = X_R{\cdot}X'_R$ (X'_R is the transposed of X_R) and Y is the matrix of the new coordinates of the data points. The new axes are known as principal axes or principal components scores. The ordination is a success if a large proportion of the total dispersion of the data is parallel with the first one, two or three principal axes. The first principal axis is oriented in such a way that the variance of the n first principal component scores is as great as possible. After PCA each point has as coordinates not the value of each measured variable for each sample but variously weighted sums of all the variables for each of the sample. The elements of the matrix U are the weights and, according to their values, it is possible to determine which properties have the highest influence in each principal component. Our data required standardization since the different properties were measured in non-comparable units. In order to do that the original data (x_{ij}) was centred (transformed to deviation from the respective mean of the values of each i property for the js sample (x_i)) and then standardized by dividing the centred data by the standard deviation of the values of the corresponding i property for the js sample (σ_i) by applying the following calculations to each element of the original data matrix: $(x_{ij} - x_i)/\sigma_i$.

3. Results and discussion

3.1. Fatty acid composition of the used oils

Table 1 shows the fatty acid composition of the TG samples (O, S, and W) as well as two reference samples (HOP and NP) used in this study. Oleic acid (C18:1) was the predominant fatty acid (FA) in O, followed by palmitic (C16:0) and linoleic (C18:2) acids in a decreasing order. In S and W, linoleic was the most abundant fatty acid, followed by oleic acid. Palmitic acid and linolenic acid (C18:3) were the third most abundant fatty acids in S and W, respectively. HOP had the highest (>78%) content of oleic acid, whereas NP presented similar amounts of both oleic and linoleic acids. These results were consistent with those reported in the literature [14,16].

3.2. Surface pressure–mean molecular area isotherms

Surface pressure–mean molecular area (π–Mma) isotherms of pure dpPC and TGs (O, S and W) are shown in Fig. 1 where dotted lines indicate the collapse pressure (π_c) and minimal molecular area (A_{min}) determination. The dpPC π–Mma isotherm showed the typical bi-dimensional liquid expanded–liquid condensed (LE–LC) phase transition at 6 mN/m and 78 Å^2/molecule, a collapse pressure at 58 mN/m and a minimal molecular area of 40 Å^2/molecule. These values were an indication of the good quality of the measuring system. On the other hand, pure O samples (corresponding to $x_O = 1$) also formed coherent monomolecular layers when they were spread at the air–water interface. Upon compression π increased smoothly leading to a π–A compression isotherm of a liquid expanded characteristic which was supported by its compressional modulus (see below) at the collapse point, $K_{c,O} = 58.3 \pm 1.6$ mN/m, which was well defined and occurred at $\pi_{c,O} = 13.1 \pm 0.11$ mN/m and $A_{min,O} = 84 \pm 2$ Å^2/molecule. A qualitative similar behavior was observed in the case of S and W. All TGs samples exhibited a slow π increase that evolved to a plateau immediately after the collapse point. The mechanism of these types of collapses, that may start at low or high surface pressures, is explained by the slow nucleation and growth of multilayer islands occurring homogeneously dispersed over the monolayer [17].

The molecular parameters of S and W monolayers are synthesized in Table 1. Collapse pressures ($\pi_{c,S} = 12.4 \pm 0.16$ mN/m and $\pi_{c,N} = 12 \pm 0.11$ mN/m) reflected a similar interfacial stability between S and W which in turn were slightly lower than that O. The minimal molecular areas of O, S and W followed the same sequence as DBI. This behavior followed that of the DBI (compare the sequence $DBI_O < DBI_S < DBI_N$) suggesting that it may be mainly influenced by the growing proportion of the unsaturated FA (C18:2 and C18:3) in the sequence O < S < W and leaded to a same sequence in the tendency to the expansion of the molecular arrangement, as reflected by compressibility moduli (K). Other compositional parameters were defined (Table 1) which, applied to multivariate analysis, contributed to define surface behavior predictors (see below).

3.3. Surface pressure–area and compressibility modulus–area isotherms of pseudo-binary dpPC–oil mixtures

Surface pressure–mean molecular area isotherms (π–Mma) of dpPC–O mixtures with x_{TG} ranging between 0 and 1 are depicted in Fig. 2a.

Values of compressibility modulus (K) as a function of molecular areas (Fig. 2b) were calculated from the π–Mma isotherms data shown in Fig. 2a, using Eq. (6) [18]:

$$K = -(A_\pi)\left(\frac{\partial \pi}{\partial A}\right)_\pi \tag{6}$$

where A_π is the molecular area at the indicated surface pressure. Because molecular areas were mean values, this parameter reflected qualitatively the physical state and the bi-dimensional phase transition of the studied monolayers. Higher values of K corresponded to lower values of interfacial elasticity. From a systematic analysis of π–Mma isotherms [19,20], it was concluded that the compressional modulus of solid condensed states are characterized by values from 1000 to 2000 mN/m, varying between 100 and 250 mN/m for liquid condensed films, while liquid expanded states showed values between 12.5 and 50 mN/m. This clearly allows concluding that TGs were in a liquid expanded state (Fig. 2b, Table 1). The compressibility of the phospholipids–TG mixtures were found between the liquid expanded state of TGs and the liquid condensed of the PCs. Maxima in K curves were found both at the mid-point of monolayers phase transitions (K_T) and at collapse points (K_c). Fig. 2b shows K–Mma isotherms calculated for each of the dpPC–O mixtures. In the case of $x_O = 0$ (pure dpPC) at the typical LE–LC bi-dimensional phase transition, occurring at $\pi = 8.2$ mN/m a $K_T \approx 25$ mN/m was observed, and at the collapse point the K_c

Author's personal copy

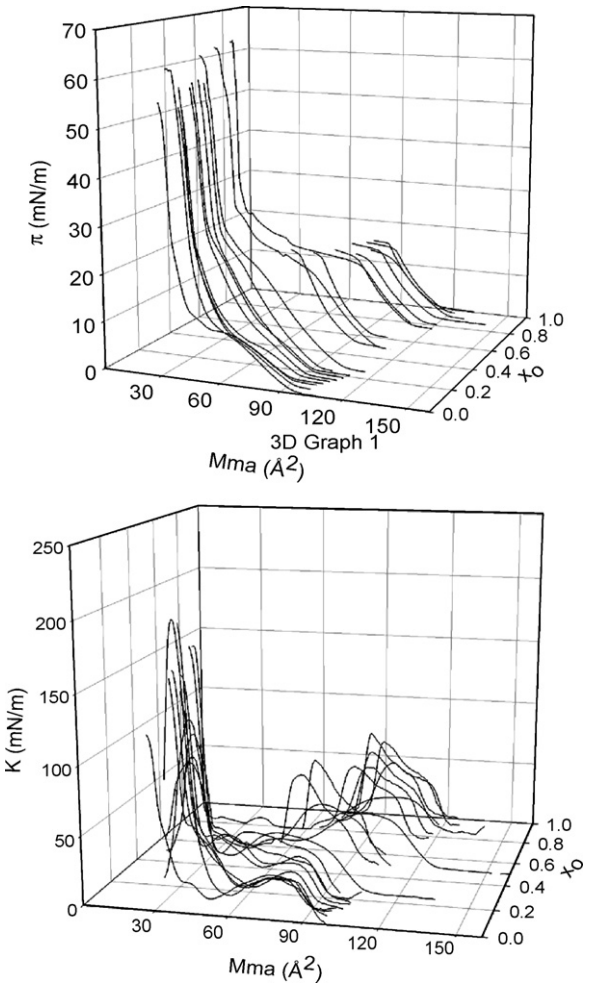

Fig. 2. Surface behavior of dpPC/olive oil mixtures. (a) π–Area isotherms of dpPC, olive (O) oil and their mixtures ranging from 0 to 1 x_O mole fraction. (b) Compressional modulus (K) of dpPC/O mixtures calculated by Eq. (6), from the isotherms shown in (a).

value (≈240 mN/m) reflected the LC characteristics of the monolayer. For the O–dpPC mixtures, as the O content increased, the bi-dimensional phase transition and the $K_c \approx 25$ mN/m were maintained up to $x_O = 0.2$. At the monolayer collapse point the K_c diminished progressively as x_O increased and at $x_O = 1$ the monolayer acquired a liquid expanded state with $K_c \approx 50$ mN/m.

Location of the phase transition mid-points and collapse points through maxima in the K–Mma curves allowed to build-up the π_{trans}–x_{TG} or π_c–x_{TG} phase diagrams of dpPC/TGs and EPC/TGs pseudo-binary mixtures (Figs. 3 and 4).

3.4. Surface pressure-composition (π_T–x_{TG} and π_c–x_{TG}) phase diagrams

Fig. 3 shows the phase diagrams of lateral pressures (π_T or π_c vs. x_{TG} (a–c) and compressional moduli (K_T or K_c) vs. x_{TG} (d–f) for dpPC/O, dpPC/S and dpPC/W mixtures.

dpPC/O mixtures exhibited full miscibility up to an olive oil molar fraction $x_O = 0.15$ with a phase transition at π_T decreasing from 6 to 4.5 mN/m and a x_O-dependent π_C which varied between 58 and 53 mN/m. The bi-dimensional phase transition was observed up to $x_O = 0.2$. The full miscibility between dpPC and O was observed below 13.1 N/m and within the whole compositional range. At higher surface pressures and $x_O \geq 0.15$ the dpPC/O system showed a partial miscibility. A monolayer phase enriched in O collapsed with a π_C decreasing continuously from 22.5 to 13 mN/m as a function of x_O. Above this π_C, the collapsed phase remained in the system in equilibrium with a monolayer phase enriched in dpPC. The latter collapsed at a π close to the π_C of dpPC.

From the analysis of compressional modulus (Fig. 3d) it can be concluded that, upon increasing the proportion of O, the film exhibited a decrease in its coherence although it remained within a LC phase state. This conclusion is supported by the smooth K decrease from 260 to 150 mN/m at high pressures. At the bottom of the phase diagram, the different phase changes described above (bi-dimensional phase transition and partial collapse) occurred between LE states of varied molecular cohesion (K varied within the 0–50 mN/m range).

The behaviors of dpPC/S (Fig. 3b and e) and dpPC/W (Fig. 3c and f) mixtures were qualitatively similar to that of the dpPC/O mixture. The main difference between these mixtures was the particular solubility of each TG in dpPC. The dashed line that crosses vertically panels a–c along the x_O corresponding to the solubility of O (S_O) in the dpPC phase evidenced the following sequence of solubilities: $S_O > S_W > S_S$.

The behavior of the EPC mixtures with O, S and N (EPC/O, EPC/S and EPC/W) (Fig. 4) was similar to that of dpPC/O however, the formers showed no bi-dimensional phase transition, the full miscibility region was wider (form $x_O = x_W = 0.15$ and $x_S = 0.20$) (Fig. 4a–c) and the film elasticity (Fig. 4d–f), on average, was higher than those of dpPC/TG mixtures. $K_{EPC/O}$ decreased from 100 to 45 mN/m within the range $0 \leq x_O \leq 0.25$ and remained nearly constant at higher x_O. The behavior of EPC/S and EPC/W mixtures (Fig. 4b, c, e, and f) were qualitatively similar to that of EPC/O. The dashed line that crosses vertically panels a–c along the x_O corresponding to solubility of O (S_O) in the EPC phase evidenced the following solubilities sequence $S_O \cong S_W < S_S$.

Generalizing, at $x_O \cong 0.2$ and above, dpPC/TG and EPC/TG phase diagrams exhibited two regions separated by a line joining the π transition points the values of which decreased with increasing x_{TG}. The upper limit of the upper region was a π value similar to the PC π_c (either EPC or dpPC according to the mixture). This behavior at $x_{TG} > 0.2$ of immiscibility at high pressures and full miscibility at low pressures is compatible with an eutectic mixture. At the lower collapse point, TGs started to separate from the mixed monolayer and formed a bulk phase (TG liquid). At the higher collapse point, another component (PC) was segregated from the monolayer to form a different bulk phase (bilayer). The remaining monolayer was in equilibrium with the two bulk phases (eutectic mixture) [21].

Alternatively, it can be interpreted that a single mixed monolayer phase is stable at π bellow the π_T's joining line and, above this π values, it collapsed forming a non-monolayer phase that coexisted with a PC enriched monolayer. At $\pi > \pi_{C,TG}$, TGs and PCs were miscible at all proportions. This is supported by the x_{TG} dependent partial collapse. Solubilities of all the studied TGs were significantly higher in EPC than in dpPC. The increase in the proportion of the long-chain length fatty acids (C20 and C22) composition correlated with a decrease of TG solubility in dpPC and an increase in EPC. The stronger effect of TGs at disrupting the molecular packing of dpPC, which is a pure substance, compared with EPC, which is a complex mixture, may account for this difference in qualitative terms. On the other hand, there was no parallelism between, e.g. DBI and solubility (see Table 1). This result highlighted the concept that the molecular organization at the supramolecular level is an emergent property that cannot be linearly derived from the molecular composition.

The line joining equilibrium points between mixed monolayer and TG liquid phase (Figs. 3a–c and 4a–c) could be fitted to Eq. (7) [21], where A_{TG} is the molecular area of TG at each π, k is the Boltzmann constant, T the absolute temperature and f_{TG} the thermodynamic activity coefficient of TGs in mixtures with each

Author's personal copy

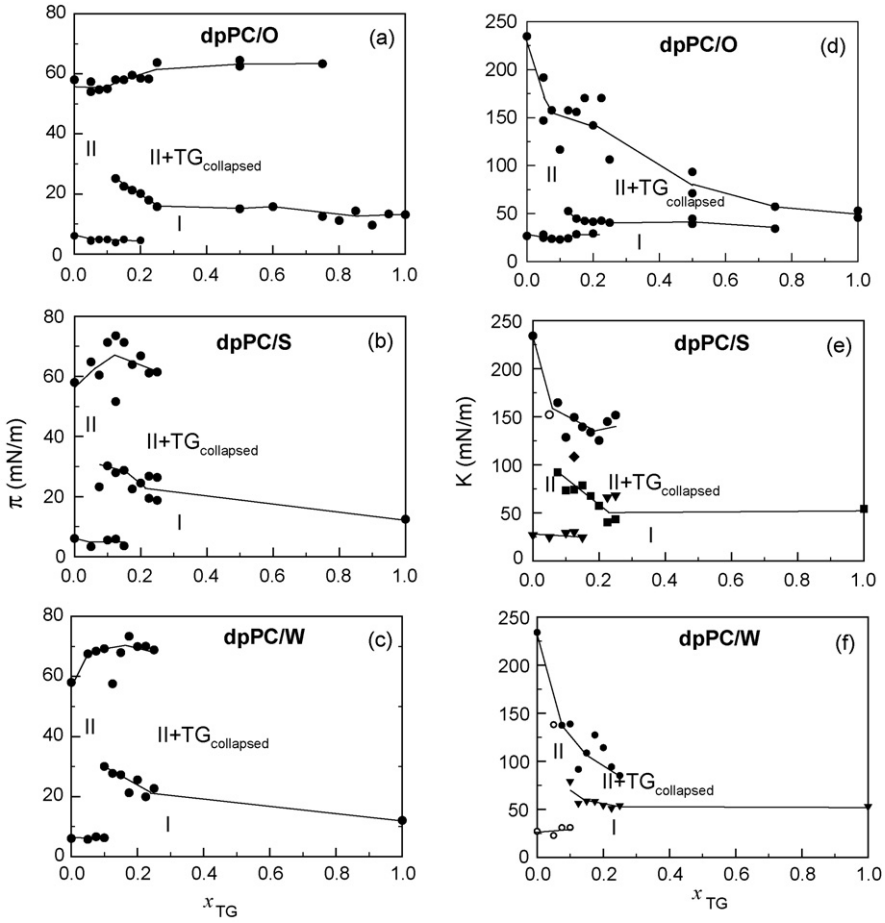

Fig. 3. Bi-dimensional phase diagrams of dpPC–TG pseudo-binary mixtures. Collapse (π_c) and transition (π_T) surface pressures (a–c) and the corresponding compressional moduli (K) (d–f) were plotted as a function of composition. The latter was expressed as TG mole fraction (x_{TG}) using the TG mean molecular mass of O, S or W. (a and d) dpPC/O, (b and e) dpPC/S and (c and f) dpPC/W mixtures. K values were determined from maxima in the K–Mma curves (e.g. in Fig. 2b for dpPC/O mixture). Full lines were drawn to schematically illustrate the limits between laterally separated phases. The dashed line crosses vertically panels a–c along the x_O corresponding to the O solubility in the dpPC phases I and II are mixed liquid-expanded (LE) and liquid-condensed (LC) bi-dimensional phases, respectively. At high π and x_{TG} the monolayer phase was in equilibrium with an excess of a collapsed TG excluded from the monolayer.

x_{TG}.

$$\int_{\pi_{c,TG}}^{\pi} A_{TG} d\pi = -kT \ln(f_{TG} x_{TG}) \quad (7)$$

Then, from the Bragg–Williams equation (Eq. (8)) lateral interaction values (ω) were calculated (Table 1).

$$\ln f_{TG} = \omega(1 - x_{TG})^2 \quad (8)$$

It is interesting to note that ω quantitatively synthesized the magnitude of deviations from the ideal behavior and the values obtained for the pseudo-binary W/EPC mixtures were of the same order of magnitude as those determined for triolein–EPC [21].

3.5. Analysis of the Mma–x_{TG} plots

The Mma–x_{TG} diagrams, at 5 and 10 mN/m showed negative deviations from ideality for dpPC/O (Fig. 5a and b) and positive deviation for EPC/O (Fig. 5c and d) and no deviations for the rest of the studied mixtures (Fig. 6). Only the mixture with the less saturated TG (O in the present work having a DBI = 0.9054) could be condensed by a lipid bearing saturated hydrocarbon chains (dpPC, DBI = 0) and expanded by lipids bearing unsaturated fatty acids (EPC, DBI = 0.837).

3.6. Thermodynamic analysis of pseudo-binary mixtures

A detailed thermodynamic analysis of surface mixing properties of the studied mixtures showed an excess Gibbs free energy (ΔG_{ex}) within the whole range of x_{TG} in EPC/TG mixtures (Fig. 7). This indicated that intermolecular repulsive forces in the mixed monolayers took place in the instabilization of the films. If the values of ΔG_{mix} and the Gibbs free energy of mixtures in ideal conditions (ΔG_{id}) were compared (Fig. 7), it became clear that at low x_{TG} the contribution of these repulsive forces (ΔG_{ex}) to the whole thermodynamic stability of the films were low ($\Delta G_{mix} = \Delta G_{ex} + \Delta G_{id}$). At $x_{TG} > 0.25$ the contribution of ΔG_{ex} to the ΔG_{mix} became more positive for the TGs containing the more unsaturated fatty acids. In the case of dpPC/O all deviations from ideality were small and negative.

3.7. Correlation analysis on TG blends formulated to exhibit a continuous variation in DBI

In order to obtain TGs monolayers with DBI values between that of O ($DBI_O = 0.9054$) and S ($DBI_S = 1.5409$), mixtures containing varying proportions of these TG (named TG_{mix}) were prepared, and a DBI_{mix} was calculated for each mixture as the weighted average of individual DBIs. Also, two additional TGs, with DBI between those of O and S, Normal Peanut (NP) (DBI = 1.19) and High Oleic Peanut

Author's personal copy

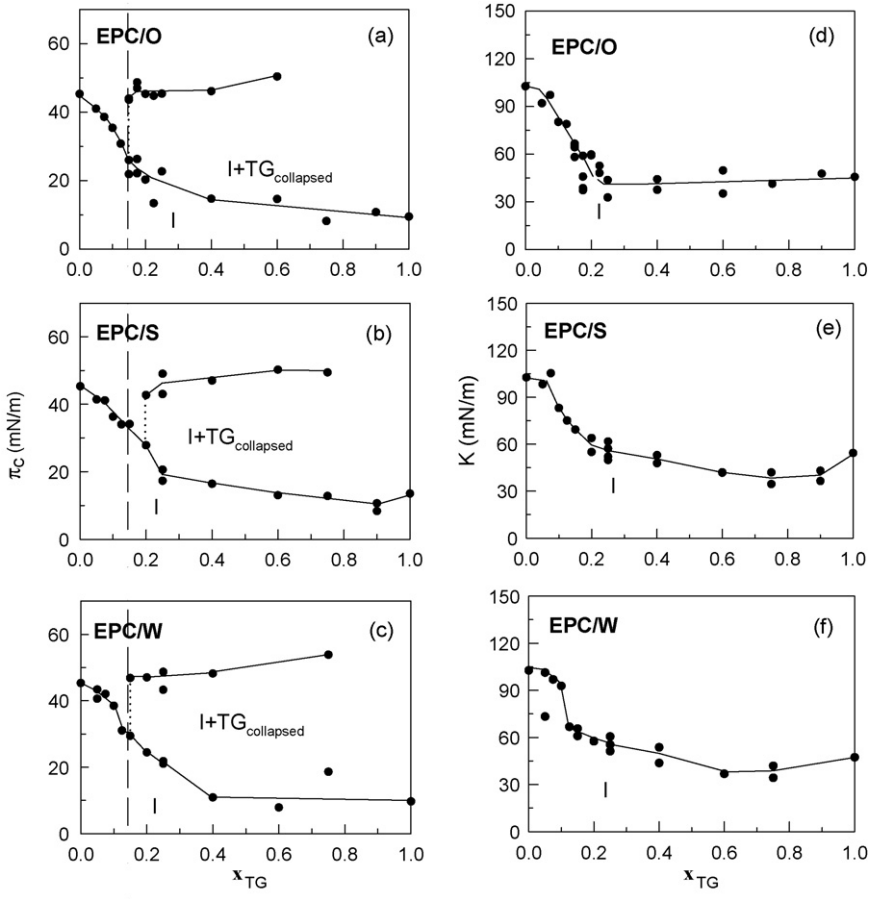

Fig. 4. Bi-dimensional phase diagrams of EPC–TG pseudo-binary mixtures. Collapse (π_c) and transition (π_T) surface pressures (a–c) and the corresponding compressional moduli (K) (d–f) were plotted as a function of composition. The latter was expressed as TG mole fraction (x_{TG}) using the TG mean molecular mass of O, S or W. (a and d) EPC/O, (b and e) EPC/S and (c and f) dpPC/W mixtures. K values were determined from maxima in the K–Mma curves (e.g. in Fig. 2b for dpPC/O mixture). Full lines were drawn to schematically illustrate the limits between laterally separated phases. The dashed line crosses vertically panels a–c along the x_O corresponding to the O solubility in the EPC phase. Region I in the phase diagrams corresponding to a mixed liquid-expanded (LE) bi-dimensional phase. At high π and x_{TG} the monolayer phase was in equilibrium with an excess of a collapsed component (TG) excluded from the monolayer.

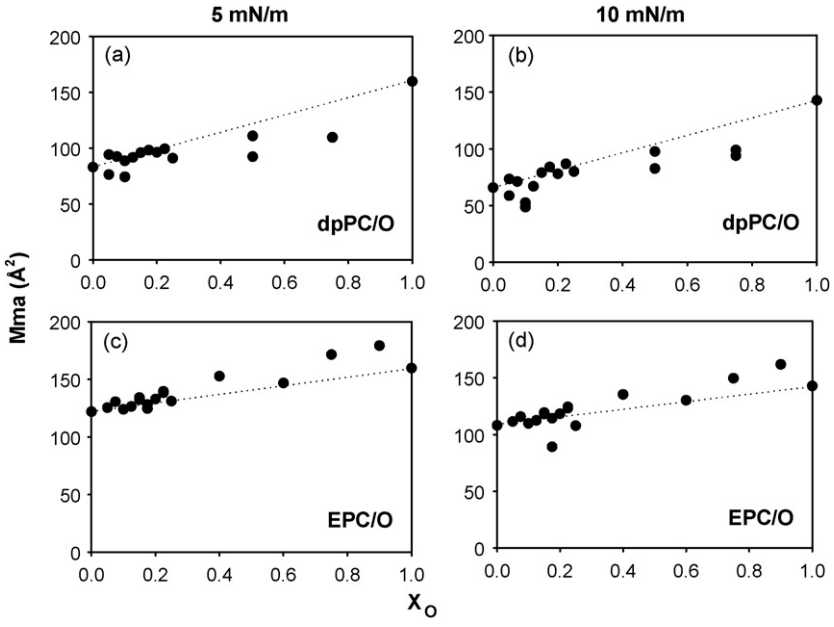

Fig. 5. Mma of PC/O mixtures deviation from the ideal behavior at a constant lateral surface pressure of 5 mN/m (a and c) and 10 mN/m (b and d). (a and b) dpPC/O mixtures, (c and d) EPC/O mixtures. Dotted lines represent states of theoretical ideal mixing or complete immiscibility.

Author's personal copy

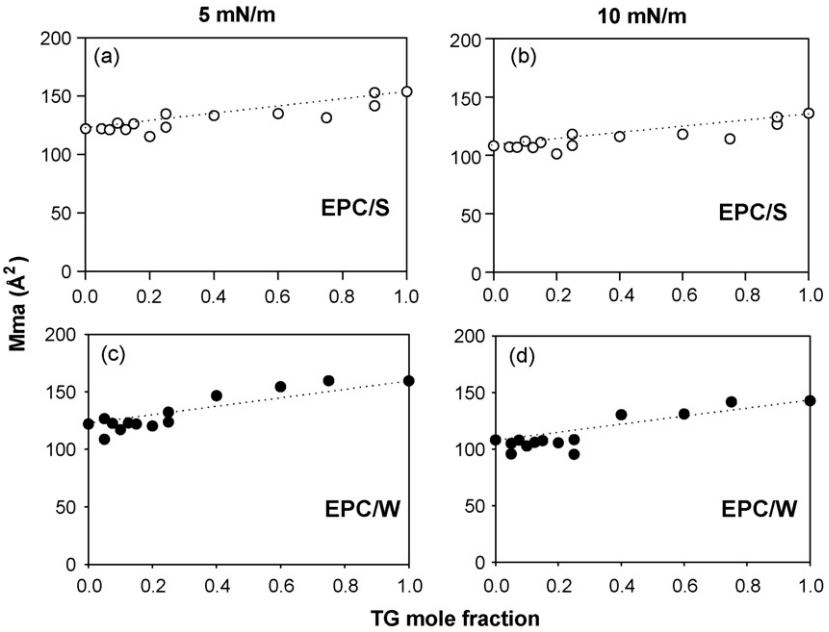

Fig. 6. Mma of EPC/TG mixtures deviation from the ideal behavior at constant lateral surface pressure of 5 mN/m (a and c) and 10 mN/m (b and d). (a and b) EPC/S mixtures and (c and d) EPC/W mixtures. Dotted lines represent states of theoretical ideal mixing or complete immiscibility.

(HOP) (DBI = 0.944), were evaluated. These oils were obtained by the same procedure applied for the other oils (see Table 1 for their composition and parameters). Compression isotherms of monolayers composed of NP or HOP either alone or mixed with EPC ($x_{EPC} = 0.25$) were recorded and their Mma at 10 mN/m and collapse pressures (π_C) were analyzed. It is important to note that, for DBI calculation, contributions of the fatty acids sterified in EPC were taken into account. A similar rationale was followed for C16/C18 calculation.

For TG_{max}–PC mixtures, deviations from ideality (DI) of their Mma at particular lateral pressures were calculated as follows:

$$DI = A_M - \left[\frac{(A_O \times \%O + A_S \times \%S)}{100} \times 0.75 + A_{EPC} \times 0.25\right] \quad (9)$$

where A_M stands for the Mma of the TG_{mix}:EPC (0.75:0.25) mixture, A_O and A_S are the Mma of O and S, respectively, *%O* and *%S* are the percentage of each oil in the TG_{mix} and A_{EPC} is the Mma of EPC. In the case of NP and HOP, the term $(A_O \times \%O + A_S \times \%S)$ was replaced by A_{NP} and A_{HOP} (Mma values for each pure oil).

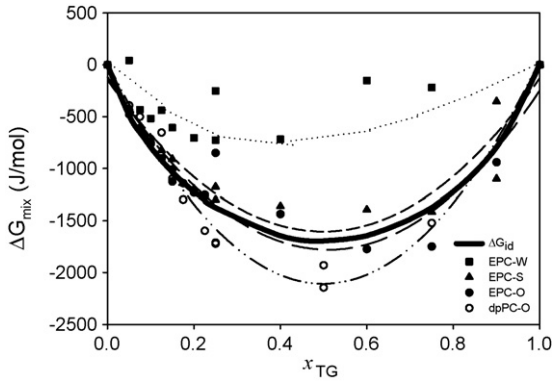

Fig. 7. ΔG_{mix} vs. x_{TG} of PC/TG mixtures. The solid line representing ΔG_{id} vs. x_{TG} was calculated from Eq. (4). Points represent ΔG_{mix} calculated using Eq. (5) within the integration limits 2 and 9 mN/m, from isotherms at each x_{TG} of the indicated PC/TG mixtures. In mixtures containing S and O, dashed lines resulted from non-linear regression analysis of experimental data. A strong positive deviation (■) and a weak negative deviation (○) from the ideal behavior can be observed for EPC/W and dpPC/O mixtures, respectively.

In Fig. 8a π_C of TG_{mix} and EPC/TG_{mix} mixtures were plotted as a function of C16/C18 and a good positive correlation was found within the whole data set studied including samples with or without EPC (correlation coefficient $R = 0.8048$). Moreover, the π_C of RP and HOP either with or without EPC, fell on the correlation line.

On the other hand, π_C decreased as a function of DBI both in the case of TG_{mix} and EPC/TG_{mix} (Fig. 8b) (note that the lower the DBI the higher the O content as compared with S content). However, contrary to what was found in the case of π_C vs. C16/C18, in the case of π_C vs. DBI the correlation was found only within each data set with $R = 0.8441$ and $R = 0.7099$ for TG_{mix} and EPC/TG_{mix}, respectively. Moreover, NP and HOP, alone or in mixtures with EPC, fell outside the correlation lines. This suggested that the fatty acid composition could impose more packing constraints than what it would have been expected just for DBI differences.

Positive deviations from the ideal behavior (DI) calculated at 5 mN/m by Eq. (9), were observed for most of the TG_{mix}, HOP and NP in pseudo-binary mixtures with EPC and, as expected, the highest deviation was exhibited by the mixtures containing not TG_{mix} but O (pure olive oil) as TG source. DI showed no correlation with C16/C18 ratio (Fig. 8c) and a weak correlation with DBI according to a second order polynomial line (Fig. 8d).

PCA was done on those variables marked with an asterisk in Table 1. The first two principal components (PC_1 and PC_2) accumulated the 93% of total variability and were characterized by the eigenvalues 5.62 and 3.65, respectively. The contributions of each variable to the corresponding PC were plotted (Fig. 9) as PC_1 vs. PC_2 (hollowed points drawn at the end of lines coming from the origin of the Cartesian plane) superimposed with points (full dots) representing the elements of the eigenvectors calculated on the samples (O, S, W, NP and HOP oils) by the use of the same data but organized in a transposed matrix. In conjunction, these data allow to recognize the grouping of NP and HOP on the one side and the rest of

Author's personal copy

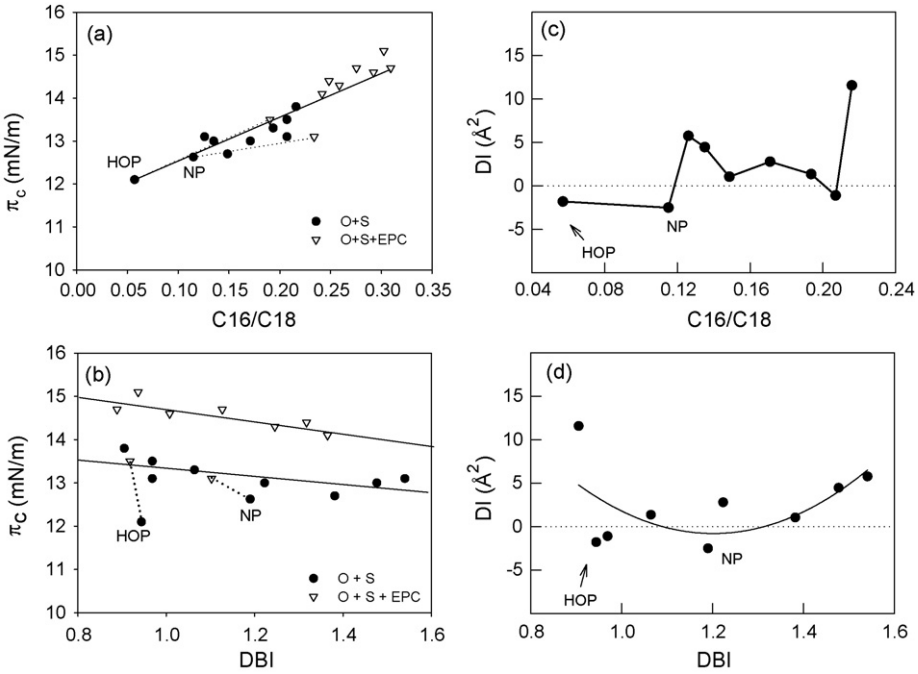

Fig. 8. Dependence of the collapse pressure (a and b) and the molecular area deviation from ideal state (c and d) on C16/C18 fatty acids ratio and DBI. Data belong to O + S artificial blends, HOP and NP, all of them alone or in mixtures with EPC (x_{EPC} = 0.75). O + S blends with $0 < x_S < 1$ were prepared to cover the desired DBI or C16/C18 ranges with or without EPC. (a and c) C16/C18 is the ratio between the total content of 16 and 18 carbon chain length fatty acids sterified in TG and in EPC. C16 and C18 were determined as the sum of the fatty acid contents of the corresponding length and at all the unsaturation levels. (b and d) DBI was calculated from Eq. (6), including (a) or not (a and d) EPC data. DI, area deviation from the ideal state at 10 mN/m. Dotted lines join NP and HOP and their corresponding pseudo-binary mixtures with EPC.

the oils on the other side. Moreover, O and S resulted more similar between them than with W (see dendrogram in Fig. 9 inset). Variables determining these differences are those that appeared closed to the corresponding sample. In example, long-chain fatty acids sterified at the glycerol backbone (reflected by $C_{20}/C_{average}$) defined the NP-HOP group, while C16/C18 and π_c separated O from W and S. These may explain the good correlation observed between π_c and C16/C18 observed in Fig. 8a for TG_{mix}–PC mixtures where the properties that are typical descriptors of O are gradually changed towards those of S.

Similar grouping behavior among oils was observed when PC's data were included in the PCA.

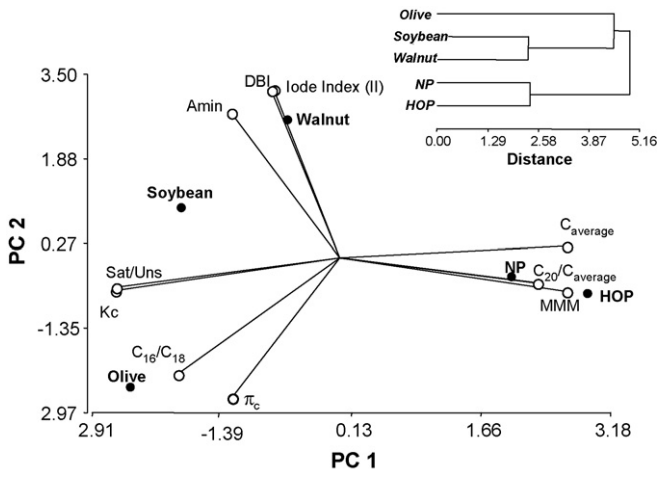

Fig. 9. Principal component analysis on compositional and surface behavioral data of O, S, W, NP and HOP triglycerides.

4. Conclusions

Collapse pressure (π_c), compressibility modulus (K) and molecular area at the closest packing (A_{min}) of vegetable oils were determined from surface pressure–mean molecular area isotherm.

The π_c-composition phase diagrams of TG–PC mixtures provided information about oils solubility limit with PCs in the monolayer phase and interaction parameters (ω) by fitting the line joining points of monolayer–$TG_{liquid\ phase}$ coexistence to a thermodynamic equilibrium model. The latters (ω values) were consistent with ΔG_{ex} and Mma deviations from ideality. From oil molar fraction values (x_{TG}) giving a $\pi_c \cong 30$ mN/m (equilibrium π of bilayers), the limiting x_{TG} allowing TGs–PCs self-assembling into vesicles was estimated, resulting higher in EPC (0.15, 0.2, 0.15 for O, S and W, respectively) than in dpPC (0.125, 0.075, 0.1). TG–EPC mixtures were in the liquid expanded stated within the whole composition and π ranges allowing a stable monolayer state. On the contrary, it was possible to found stable TG–dpPC mixed monolayers in a liquid condensed state mainly at x_{TG} below the TG solubility limit in ddPC. It is important to note that the collapsed phase that appears beyond the solubility limit of TGs in PC would consist of emulsion particles formed by a TG core covered by a PC monolayer.

Principal component analysis performed on surface parameters, grouped S and W leaving O in a separated group, mainly based on variables estimating the effect of unsaturation degree of the fatty acids sterified at TGs and A_{min} values, on the one hand, and π_c and the weighted average C16/C18 molar ratio, on the other hand. Surface parameters of independent natural oils could be interpolated in π_c–C16/C18 and A_{min}–DBI correlation lines between of O–S mixtures (TG_{mix}) or TG_{mix}–PC suggesting C16/C18 and DBI as predictors to formulate oil blends with selected surface behavior.

Hence, tuning the proportions of certain vegetable oils and phospholipids it may be possible to design the type (nanoparticles, nanofilms or emulsions) and viscosity of the self-assembled struc-

Author's personal copy

tures that are expected to be formed by these mixtures in aqueous media.

Appendix A. Supplementary data

Supplementary data associated with this article can be found, in the online version, at doi:10.1016/j.colsurfb.2009.08.014.

References

[1] F.D. Gunstone, F.B. Padley, Lipid Technologies and Applications, Marcel Dekker, New York, 1997.
[2] N. Patel, U. Schmid, M.J. Lawrence, Phospholipid-based microemulsions suitable for use in foods, J. Agric. Food Chem. 54 (2006) 7817–7824.
[3] N. Parris, R.F. Joubran, D.P. Lu, Triglyceride microemulsions: effect of nonionic surfactants and the nature of the oil, J. Agric. Food Chem. 42 (1994) 1295–1299.
[4] T.G. Redgrave, M.G. Ivanova, R. Verger, The condensing effects of egg lecithin and cholesterol on triolein monolayers are inhibited by substitution of one saturated acyl chain in the triacylglycerol, Biochim. Biophys. Acta 1211 (1994) 229–233.
[5] M. Sugiura, M. Isobe, Studies on the lipase of *Chromobacterium viscosum*. IV. Substrate specificity of a low molecular weight lipase, Chem. Pharm. Bull. 23 (1975) 1226–1230.
[6] T. Ohtsu, C. Katagiri, M.T. Kumura, S.H. Hori, Cold adaptations in drosophila. Qualitative changes of triacylglycerols with relation to overwintering, J. Biol. Chem. 268 (1993) 1830–1834.
[7] H.L. Brockman, in: B. Borgstrom, H.L. Brockman (Eds.), General Features of Lipolysis: Reaction Scheme, Interfacial Structure and Experimental Approaches in Lipases, Elsevier, Amsterdam, 1984, pp. 1–46.
[8] A.C. Teixeira, P. Brogueira, A.C. Fernandes, A.M. Goncalves da Silva, Phase behaviour of binary mixtures involving tristearin, stearyl stearate and stearic acid: thermodynamic study and BAM observation at the air–water interface and AFM analysis of LB films, Chem. Phys. Lipids 153 (2008) 98–108.
[9] G. Cevc, D. Marsh, Phospholipid Bilayers, John Wiley and Sons Inc., New York, 1987.
[10] V.M. Kaganer, H. Mhöwald, P. Dutta, Structure and phase transitions in Langmuir monolayers, Rev. Mod. Phys. 71 (1999) 779–819.
[11] J.A. Hamilton, Interactions of triglycerides with phospholipids: incorporation into the bilayer structure and formation of emulsions, Biochemistry 28 (1989) 2514–2520.
[12] L. Tobares, C.A. Guzmán, D.M. Maestri, Effect of the extraction and bleaching processes on jojoba (*Simmondsia chinensis*) wax quality, Eur. J. Lipid Sci. Technol. 105 (2003) 749–753.
[13] M. Torres, D. Maestri, Chemical composition of Arbequina Olive oil in relation to extraction and storage conditions, J. Sci. Food Agric. 86 (2006) 2311–2317.
[14] M.A. Perillo, D.M. Maestri, Surface behavior of jojoba oil alone or in mixtures with soybean oil, Colloid Surf. A: Physicochem. Eng. Asp. 256 (2005) 199–205.
[15] F. Rohlf, Numerical Taxonomy and Multivariate Analysis System, Exeter Publishing, New York, 1984.
[16] M. Torres, M. Martinez, D.M. Maestri, A multivariate study of the relationship between fatty acids and volatile flavor components in olive and walnut oils, J. Am. Oil Chem. Soc. 82 (2005) 105–110.
[17] M.A. Valdes-Covarrubias, R.D. Cadena-Nava, E. Vásquez-Martínez, D. Valdez-Pérez, J. Ruiz-García, Crystallite structure formation at the collapse pressure of fatty acid Langmuir films, J. Phys. Condens. Matter 16 (2004) S2097–S2107.
[18] J.N. Israelachvili, Intermolecular and Surface Forces, Academic Press, New York, 1989.
[19] D.C. Carrer, B. Maggio, Phase behavior and molecular interactions in mixtures of ceramide with dipalmitoylphosphatidylcholine, J. Lipid Res. 40 (1999) 1978–1989.
[20] J.T. Davies, E.K. Rideal, Interfacial Phenomena, Academic Press, New York, 1963.
[21] T. Handa, H. Saito, K. Miyajima, Eutectic mixed monolayers in equilibrium with phospholipid-bilayers and triolein-liquid phase, Biophys. J. 64 (1993) 1760–1765.